Human RECQL5 participates in the removal of endogenous DNA damage

Takashi Tadokoro, Mahesh Ramamoorthy, Venkateswarlu Popuri, Alfred May, Jingyan Tian, Peter Sykora, Ivana Rybanska*, David M. Wilson III, Deborah L. Croteau, and Vilhelm A. Bohr
Laboratory of Molecular Gerontology, National Institute on Aging, Baltimore, MD 21224

ABSTRACT **Human RECQL5 is a member of the RecQ helicase family, which maintains genome stability via participation in many DNA metabolic processes, including DNA repair. Human cells lacking RECQL5 display chromosomal instability. We find that cells depleted of RECQL5 are sensitive to oxidative stress, accumulate endogenous DNA damage, and increase the cellular poly(ADP-ribosyl)ate response. In contrast to the RECQ helicase family members WRN, BLM, and RECQL4, RECQL5 accumulates at laser-induced single-strand breaks in normal human cells. RECQL5 depletion affects the levels of PARP-1 and XRCC1, and our collective results suggest that RECQL5 modulates and/or directly participates in base excision repair of endogenous DNA damage, thereby promoting chromosome stability in normal human cells.**

Monitoring Editor
Orna Cohen-Fix
National Institutes of Health

Received: Feb 13, 2012
Revised: Aug 21, 2012
Accepted: Sep 6, 2012

INTRODUCTION

RECQ helicases comprise a highly conserved family of DNA helicases that operate to maintain genomic DNA stability in human and other cells, play diverse functions in DNA replication, recombination, and DNA repair (Brosh and Bohr, 2007; Bohr, 2008; Chu and Hickson, 2009; Singh *et al.*, 2012), and catalyze several types of DNA transactions. Defects in human RECQ helicases are associated with premature aging, genome instability, and cancer predisposition. RECQ helicase family members possess intrinsic DNA-dependent ATPase and ATP-dependent DNA-unwinding activity, with variable preferences for specific DNA structures. Human cells express five RECQ homologues—RECQL1, BLM, WRN, RECQL4, and RECQL5—whereas prokaryotes and simple eukaryotes express a single RECQ enzyme. Defects in human BLM and WRN cause the autosomal recessive diseases Bloom syndrome and Werner syndrome, respectively. Defects in RECQL4 are associated with three human diseases—Rothmund–Thomson, RAPADILINO, and Baller–Gerold syndrome (Yu *et al.*, 1996; Kitao *et al.*, 1999; Lindor *et al.*, 2000; Dietschy *et al.*, 2007). It is likely that the five human RECQ helicases have overlapping but distinct cellular functions.

RECQL5 exists in three alternatively spliced isoforms—RECQL5α, RECQL5β, and RECQL5γ (Shimamoto *et al.*, 2000)—and is the least well characterized of the five human RECQ helicases. RECQL5α (410 amino acids) and RECQL5γ (435 amino acids) localize to the cytoplasm, whereas RECQL5β (991 amino acids) localizes to the nucleus. The precise biological role of human RECQL5 is not known. Mice lacking RECQL5 show increased chromosomal instability (Hu *et al.*, 2005b, 2009), and *Caenorhabditis elegans* depleted of RECQL5 has a shorter lifespan than does wild type (Jeong *et al.*, 2003). Furthermore, the response of human colorectal cancer cells to topoisomerase I inhibitors appears to be modulated by RECQL5 (Wang *et al.*, 2011). RECQL5$^{-/-}$/BLM$^{-/-}$ double-knockdown chicken DT40 cells display decreased survival and have a higher frequency of sister chromatid exchange events than BLM$^{-/-}$ cells (Wang *et al.*, 2003). Although RECQL5 and RECQL1 appear to be rather homogeneously expressed, BLM, WRN, and RECQL4 demonstrate selective tissue-specific patterns of expression (Kitao *et al.*, 1998). These and other studies support a role for RECQL5 in DNA replication, DNA repair, homologous recombination, and RNA polymerase II (RNAP II)-mediated transcription (Hu *et al.*, 2007; Aygun *et al.*, 2008; Izumikawa *et al.*, 2008; Schwendener *et al.*, 2010).

Base excision repair (BER) is the most prominent pathway for repair of endogenous DNA damage. In the first step of BER, damaged

This article was published online ahead of print in MBoC in Press (http://www.molbiolcell.org/cgi/doi/10.1091/mbc.E12-02-0110) on September 12, 2012.

*Present address: Radiation Oncology and Molecular Sciences, Johns Hopkins University School of Medicine, Baltimore, MD 21231.

Address correspondence to: Vilhelm A. Bohr (vbohr@nih.gov).

Abbreviations used: BER, base excision repair; DSB, double-strand break; Fapy, formamide pyrimidine; GFP, green fluorescent protein; HPLC, high-performance liquid chromatography; PAR, poly(ADP-ribose); RNAP II, RNA polymerase II; SSB, single-strand break; 8-oxoG, 8-oxoguanine.

base moieties, such as 8-oxoguanine, are recognized and excised by a DNA glycosylase, resulting in an abasic site. The abasic site is then incised by apurinic endonuclease 1 (APE1), producing a single-strand break intermediate, which is in turn a substrate for DNA repair synthesis and 5′-end clean-up by DNA polymerase β (POL β), followed by nick ligation by a DNA ligase (Wilson and Bohr, 2007). The most common causes of base damage are endogenous reactive oxygen species and exogenous xenobiotic compounds. Deficient repair of oxidative DNA damage correlates with premature aging and age-related diseases (Golden *et al.*, 2002; Wilson and Bohr, 2007). Single-strand breaks (SSBs) generated by DNA-damaging agents or during processing of other types of DNA damage are also repaired by BER. SSB repair (SSBR) involving several components of the BER pathway also requires poly(ADP-ribose) polymerase 1 (PARP1; Caldecott, 2008). A large load of unrepaired SSBs contributes to genetic instability and can lead to double-strand DNA breaks (DSBs) and cell death (Heeres and Hergenrother, 2007; Caldecott, 2008).

WRN, BLM, RECQL4, and RECQL1 modulate BER in vitro and in vivo (Szekely *et al.*, 2005; Harrigan *et al.*, 2006; Schurman *et al.*, 2009; Sharma *et al.*, 2012). Consistent with this, WRN-targeted small interfering RNA inhibits repair of oxidative and alkylation DNA damage in human primary fibroblasts (Imamura *et al.*, 2002; Harrigan *et al.*, 2006). WRN helicase also stimulates the DNA strand displacement activity of POL β (Harrigan *et al.*, 2003) and single-stranded DNA flap processing by FEN1 (Brosh *et al.*, 2001). WRN helicase is inhibited by APE1 (Ahn *et al.*, 2004), interacts with NEIL1 in vivo and in vitro (Das *et al.*, 2007; Popuri *et al.*, 2010), stimulates repair of formamido pyrimidine (Fapy) lesions (Das *et al.*, 2007), and interacts with PARP1, which ribosylates a number of cellular proteins during DNA repair. PARP1 ribosylation is diminished in WRN-deficient cells, suggesting that PARP1 is activated or stimulated by WRN (von Kobbe *et al.*, 2003). BLM and RECQL4 also modulate the enzymatic activities of several BER proteins, such as APE1, POL β, ligase 3 (LIG3), and FEN1 (Sharma *et al.*, 2004a,b; Schurman *et al.*, 2009). In addition, RECQL1-deficient cells are mildly sensitive to oxidative DNA damage and hyperactivate PARP1 in response to H_2O_2 (Sharma *et al.*, 2012). Our previous studies and those of others suggest that RECQL5 may interact functionally with FEN1 during long-patch BER and/or homologous recombination and lagging-strand DNA replication (Sharma *et al.*, 2004a,b; Schurman *et al.*, 2009; Speina *et al.*, 2010) or possibly modulate transcription by RNAP II (Aygun *et al.*, 2008; Islam *et al.*, 2010; Izumikawa *et al.*, 2008; Kanagaraj *et al.*, 2010; Li *et al.*, 2011).

Recently we generated cells with stable depletion of RECQL5. They display a slow proliferation rate, G2/M cell cycle arrest, and late-S-phase cycling defects (Ramamoorthy *et al.*, 2012). We previously suggested that this phenotype is due to a defective functional interaction between RECQL5 and topoisomerase IIα (Ramamoorthy *et al.*, 2012). In the present study, we characterize the effect of short hairpin RNA (shRNA)–mediated depletion of RECQL5β (referred to in this article as RECQL5) on the repair of endogenous DNA damage in human cells. Our results show that depletion of RECQL5 sensitizes cells to oxidative stress, causes accumulation of endogenous DNA damage, and increases cellular PAR levels. Moreover, we find that RECQL5 accumulates at DNA laser-induced single-strand breaks in normal human cells. In contrast, human RECQ helicases WRN, BLM, and RECQL4 are not recruited to laser-induced single-strand breaks. Furthermore, expression of *XRCC1* and *PARP1*, which play roles in BER and SSBR, is low in RECQL5-depleted cells as compared with control cells. Collectively, our results suggest that RECQL5 promotes chromosome stability in normal human cells by playing a nonredundant and unique role in BER, specifically modulating and/or directly participating in BER-mediated repair of endogenous DNA damage.

RESULTS

RECQL5-depleted cells are hypersensitive to oxidative DNA-damaging agents

We previously showed that RECQL5 interacts and colocalizes with FEN1 in response to oxidative stress and stimulates FEN1 incision activity in a similar manner to WRN, BLM, and RECQL4 (Speina *et al.*, 2010). FEN1 is known to participate in various processes, such as homologous recombination, lagging-strand DNA replication, and long-patch BER (Lieber, 1997; Shen *et al.*, 2005; Saharia *et al.*, 2008). Other research groups demonstrated that RECQL5 is involved in homologous recombination and DNA replication (Kanagaraj *et al.*, 2006; Hu *et al.*, 2007, 2009; Schwendener *et al.*, 2010). In the present study we seek to further characterize the potential role of RECQL5 in BER and SSBR.

To investigate the in vivo role of RECQL5, we generated two HeLa-derived cell lines stably expressing shRECQL5-1 or shRECQL5-2, respectively, targeting the 3′ untranslated region or coding region of the RECQL5 mRNA, using a lentiviral system (Ramamoorthy *et al.*, 2012). HeLa cells harboring these shRNAs were harvested and RECQL5 protein levels were analyzed by Western blot. As shown in Figure 1A, RECQL5 protein levels were significantly decreased in the two knockdown cell lines (shRECQL5-1 and shRECQL5-2). To examine the effect of RECQL5 depletion on the response to oxidative stress, we measured cell viability in these cells after treatment with menadione or hydrogen peroxide and compared them with control cells. The results showed that cells expressing either shRECQL5-1 or shRECQL5-2 were more sensitive to both menadione and hydrogen peroxide than were shScrambled control cells, especially at a low dose of damaging agent (Figure 1, B and C). It should be noted that an attempt to express shRNA-resistant RECQL5 was not successful due to toxicity from overexpression (unpublished data not shown), but an off-target effect is not likely because similar effects were seen with two different shRNA constructs.

To examine further the consequence of RECQL5 deficiency, we evaluated another cell type to see whether similar phenotypes would be observed. Specifically, we measured cell survival after oxidative stress using HCT116 colorectal cancer cells expressing shRECQL5-2. We chose shRECQL5-2 because RECQL5 knockdown was more significant than the one seen for the shRECQL5-1 in HCT116 cells as well (Ramamoorthy *et al.*, 2012). As observed in HeLa cells, HCT116 shRECQL5-2 cells exhibited increased sensitivity to both menadione and hydrogen peroxide (Figure 1, E and F). Similar findings were also obtained for knockdown and control cells using a clonogenic survival assay (Supplemental Figure S1). Taken together, our results indicate that depletion of RECQL5 sensitizes cells to oxidative stress.

Accumulation of endogenous DNA damage in RECQL5-knockdown cells

In light of the aforementioned sensitivity to oxidative DNA-damaging agents, we speculated that RECQL5-knockdown cells might be deficient in some aspect of DNA repair. To investigate the in vivo role of RECQL5 in BER, we examined whether the loss of RECQL5 modulated the level of oxidatively modified bases in the genome. One of the most commonly used markers of exposure to reactive oxygen species and unrepaired oxidative DNA damage is 8-oxoguanine (8-oxo-dG; Hu *et al.*, 2005a). We measured the cellular content of 8-oxo-dG using high-performance liquid chromatography (HPLC)

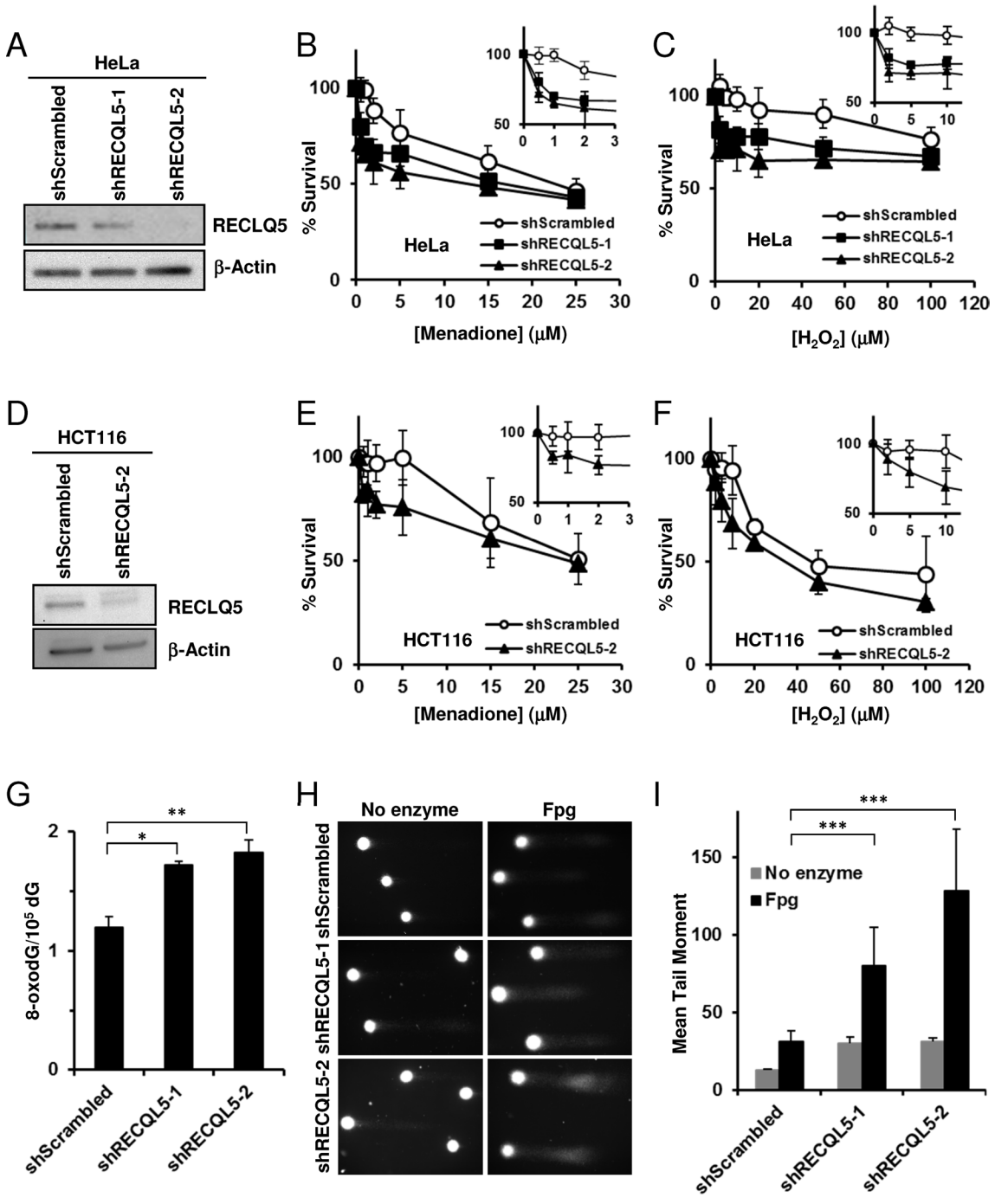

FIGURE 1: RECQL5-depleted cells show increased sensitivity to oxidative stress, accumulate endogenous DNA damage, and show reduced repair capacity. (A) Knockdown of RECQL5 in HeLa cells or (D) in HCT116 cells was confirmed by Western blot. RECQL5-depleted and scrambled control cells were plated on 96-well plates and treated with (B, E) 0, 0.5, 1, 2, 5, 15, and 25 μM of menadione or (C, F) 0, 2, 5, 10, 20, 50, and 100 μM of hydrogen peroxide. Cells were allowed to grow for 24 h, and cell viability was measured. The normalized values compared with untreated samples are represented (open circle, shScrambled; filled square, shRECQL5-1; filled triangle, shRECQL5-2). (B, C) Examined using HeLa cells stably expressing RECQL5-targeting shRNAs. (E, F) Examined using HCT116 cells stably expressing RECQL5 targeting shRNA. (G) Measurement of 8-oxo-dG in DNA derived from RECQL5-knockdown and control cells. Cells were harvested after 2 d of selection, and DNA samples were prepared as described in *Materials and Methods*. At least two biologically independent experiments were performed, and error bars represent ± SD. The indicated *p* values were analyzed with Student's *t* test ($n = 2$). *$p < 0.001$, **$p < 0.01$. (H) Comet assays of RECQL5-depleted and control cells untreated or treated with Fpg enzyme to detect endogenous DNA base damage. Representative images of nuclear DNA. (I) The results of quantitative measurements of endogenous DNA damage (Tail Moments). The results in the absence of Fpg are shown by gray bars, and those in the presence of Fpg are shown by black bars. At least >100 nuclear DNAs were analyzed in each experiment. Two biologically independent experiments were performed, and error bars represent ± SD. The indicated *p* values were analyzed with Student's *t* test ($n = 2$). ***$p < 0.05$.

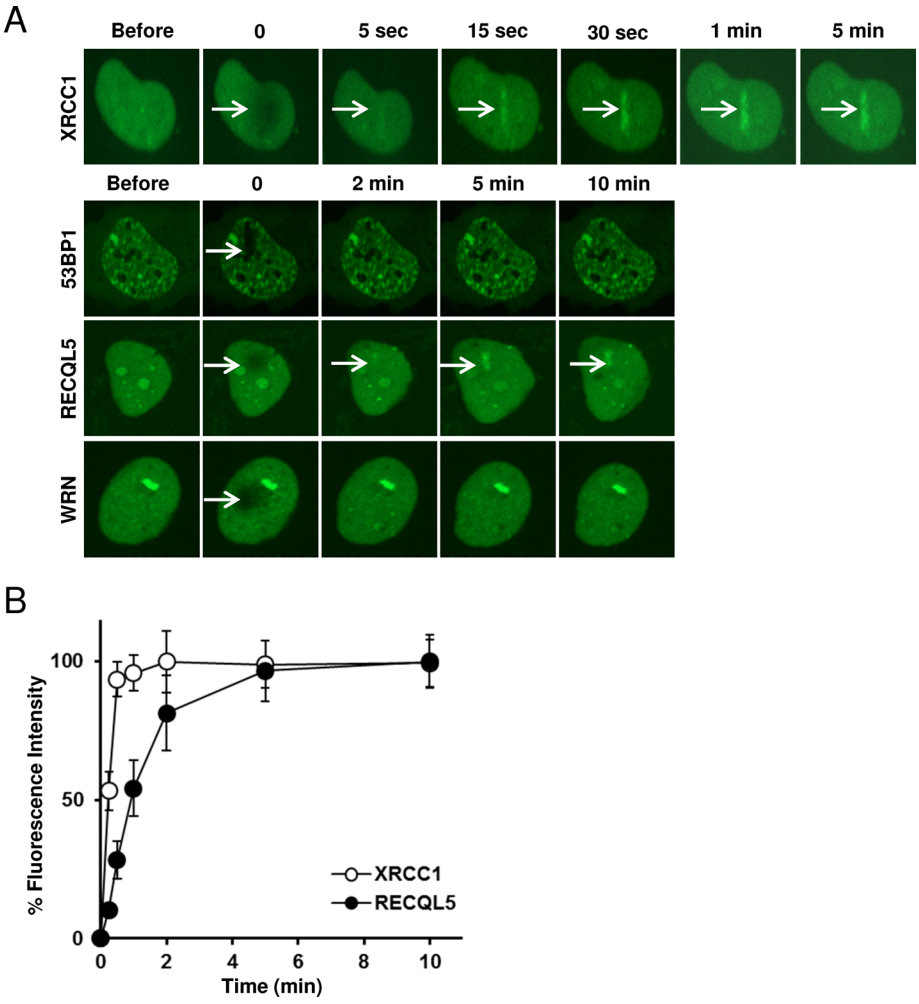

FIGURE 2: GFP-RECQL5 is recruited to the 3% laser–irradiated sites. (A) The association of GFP-XRCC1, 53BP1, RECQL5, and WRN proteins is shown at different time intervals after microirradiation. HeLa cells were transfected with GFP-tagged RECQL5, WRN, 53BP1, or XRCC1 plasmids. At 24 h posttransfection, the cells were laser microirradiated within the nucleus with 435-nm laser light at 3% laser intensity. The images were captured for 60 s through fluorescence recovery after photobleaching channel using confocal microscopy. Arrow represents the site of laser irradiation. (B) The normalized intensity values of the kinetics of association of different proteins. Fluorescence intensity derived from GFP-fusion proteins was measured using Volocity-5 software. Measured values were normalized using the highest intensities derived from GFP-RECQL5 or XRCC1 as 100%. The recruitment of GFP-XRCC1 is indicated with open circles, and that of GFP-RECQL5 is indicated with filled circles. Approximately 10 cells were examined in each experiment.

with electrochemical detection (Shigenaga *et al.*, 1990; Anson *et al.*, 2000). The results indicate that shRECQL5-1– and shRECQL5-2–knockdown cells accumulated 1.4- or 1.5-fold more 8-oxo-dG lesions than did the shScrambled control cells (Figure 1G).

As an independent measure of endogenous DNA damage, we used the alkaline comet assay to determine whether the loss of RECQL5 affected the level of formamido pyrimidine DNA glycosylase (Fpg)–sensitive DNA modifications. HeLa shRECQL5-1 and shRECQL5-2 cells were used, and the experiments were performed in the presence or absence of *Escherichia coli* Fpg, which incises DNA at oxidized guanine bases or abasic sites, thereby creating a single-strand break. The mean tail moment was ~2.3- and 2.4-fold higher in shRECQL5-1 and shRECQL5-2 knockdown cells, respectively, than in shScrambled control cells without Fpg treatment (Figure 1, H and I), and 2.5- and 4-fold higher in shRECQL5-1– and shRECQL5-2–knockdown cells ($p < 0.05$) when the nuclei were treated with Fpg (Figure 1, H and I). These results demonstrate that strand breaks and alkaline/Fpg–sensitive sites, including Fapy and 8-oxo-dG, as well as abasic sites, are more abundant in RECQL5-knockdown cells than in the shScrambled control cells.

RECQL5 accumulates at laser-induced SSBs

To analyze whether and at what stage RECQL5 might be involved in BER/SSBR, we used confocal laser scanning microscopy to localize green fluorescent protein (GFP)–tagged RECQL5 in cells carrying site-specific, laser-induced single-strand breaks (SSBs; Lan *et al.*, 2005; Karmakar *et al.*, 2006; Mailand *et al.*, 2007; Haince *et al.*, 2008; Yano *et al.*, 2008; Singh *et al.*, 2010; Popuri *et al.*, 2012). In this experiment, SSBs were induced in HeLa cells using a 435-nm laser at 3% intensity. These conditions induce SSBs in DNA rather than double-strand breaks (DSBs) because we detect recruitment of GFP-tagged XRCC1 but not of GFP-tagged 53BP1 (indicating absence of DSBs; Figure 2A). Figure 2A shows an increase in GFP-RECQL5 foci at the laser-induced strand breaks but no increase of GFP-WRN. Previous studies also showed that WRN, BLM, and RECQL4 are not recruited to laser-induced SSBs (Singh *et al.*, 2010). Thus recruitment of RECQL5 to SSBs may be unique among human RECQ helicases. Of interest, kinetic experiments showed that XRCC1 is recruited to laser-induced SSBs within ~30 s, whereas RECQL5 foci reached a maximum fluorescence ~5 min postirradiation (Figure 2B). This suggests that RECQL5 may not be required during the SSBR recognition phase but may instead play a role during a later step of this DNA damage–processing pathway.

The kinetics of formation of GFP-XRCC1 foci was also examined in laser-irradiated HeLa cells expressing shRECQL5-1, shRECQL5-2, or scrambled shRNA (shScrambled; see Western blot; Figure 3A). Under these experimental conditions, the kinetics of XRCC1 foci formation was independent of the level of expression of RECQL5. However, the kinetics of XRCC1 foci dissociation was delayed in both RECQL5-knockdown cells, requiring 5 h in shRECQL5-1 and 6 h in shRECQL5-2 but only 2.5 h in shScrambled cells (Figure 3, B and C). These results, which are consistent with the results of the alkaline comet assay (Figure 1, H and I), suggest that SSBR is less efficient in RECQL5-knockdown cells.

Poly(ADP-ribosyl)ation in response to DNA damage

PARP1 plays a critical role in SSBR. Thus, in cells carrying SSBs, PARP1 undergoes rapid activation, after which the polymerase adds poly(ADP-ribose) (PAR) to itself and other SSBR proteins, including

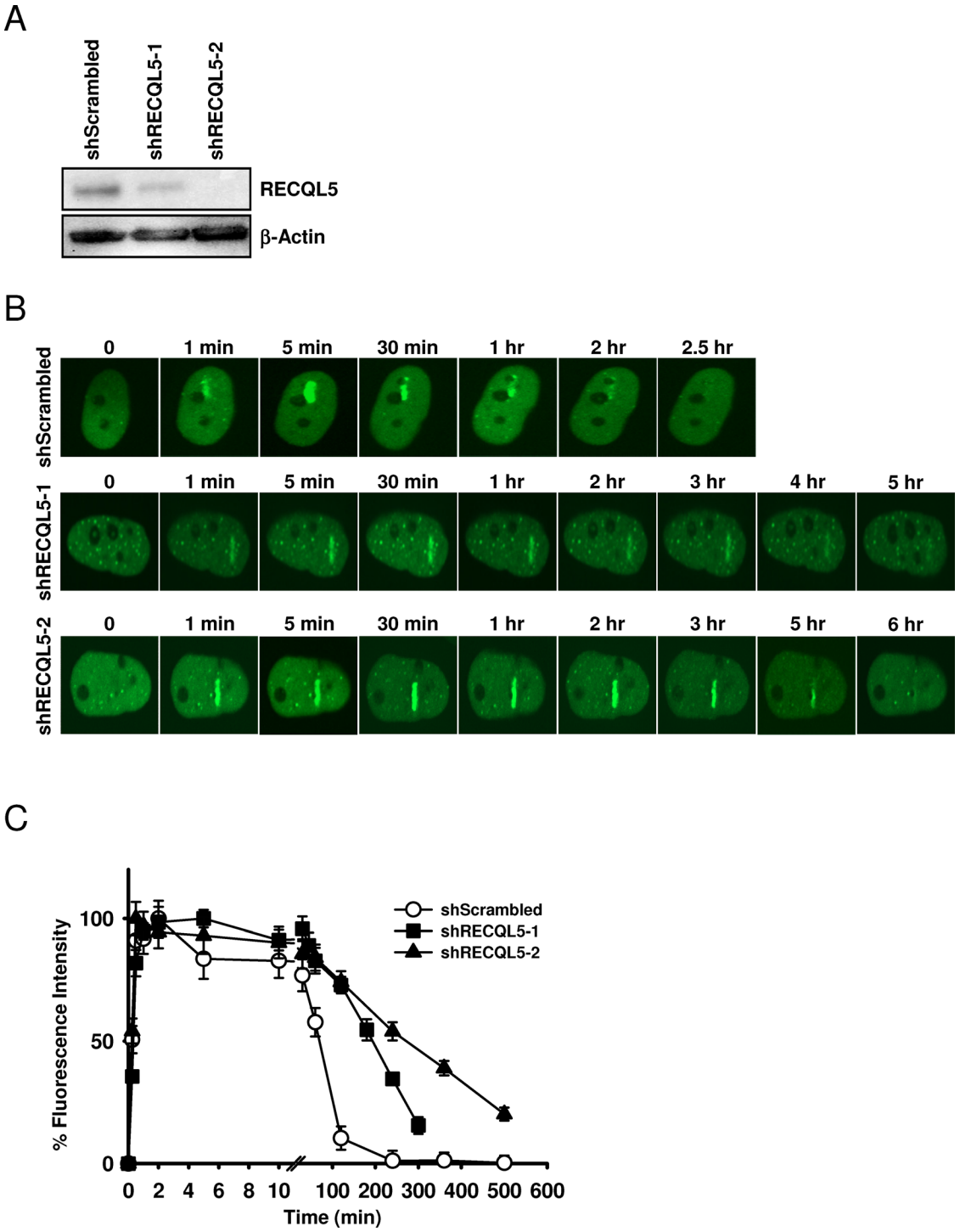

FIGURE 3: GFP-XRCC1 accumulates longer at the laser-irradiated sites in RECQL5-deficient cells. (A) RECQL5 knockdown was confirmed by Western blot. (B) The association of GFP-XRCC1 in shScrambled control cells, shRECQL5-1 cells, and shRECQL5-2 cells is shown at different time intervals after microirradiation. Either RECQL5-depleted or scrambled control cells were transfected with GFP-XRCC1 plasmid, and the recruitment kinetics of GFP-XRCC1 was analyzed with the same procedure described in the legend to Figure 2. Laser irradiation condition was same as the experiment in Figure 2. (C) The normalized intensity values of the kinetics of association of XRCC1. Fluorescence intensity at the site was measured using Volocity-5 software. Obtained intensity is normalized using the highest intensities derived from XRCC1 as 100%. The kinetics of XRCC1 in control cells is shown by open circles and that in shRECQL5-1 and shRECQL5-2 cells by solid squares and solid triangles, respectively.

XRCC1 (Masson *et al.*, 1998; Pleschke *et al.*, 2000). We previously showed that PARP1 activity on target protein substrates, but not self-modification, is impaired in WS primary fibroblasts (von Kobbe *et al.*, 2003), suggesting that PARP1 ribosylation activity is regulated by WRN protein. A recent report shows that RECQL1-depleted cells hyperactivate PARP1 specifically in response to H_2O_2 treatment and

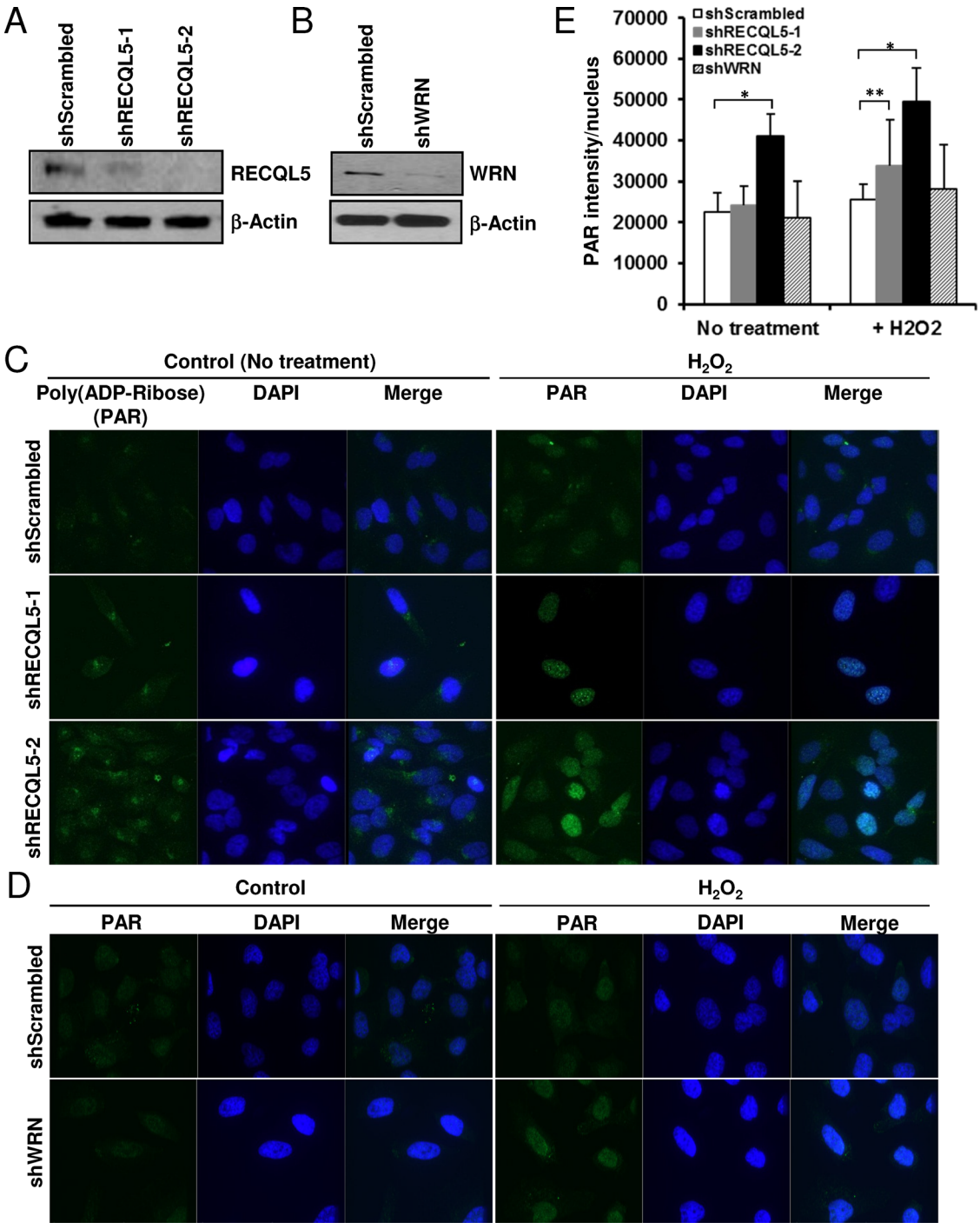

FIGURE 4: PAR immunoreactivity is increased in RECQL5-depleted cells. Knockdown of RECQL5 (A) and WRN (B) were confirmed by Western blot. (C) Left, representative immunofluorescence images of HeLa shRECQL5-1 and shRECQL5-2 without H_2O_2 treatment; right, those with H_2O_2 treatment. H_2O_2-treated or untreated RECQL5-depleted and control cells were fixed and probed with anti-PAR antibodies. (D) Left, representative immunofluorescence images of HeLa shWRN without H_2O_2 treatment; right, those with H_2O_2. WRN-depleted cells were also examined with the same procedures as for RECQL5-depleted cells. (E) Quantification of PAR immunoreactivity in C and D. Fluorescence intensity–derived PAR antibody was measured using Volocity-5 software. PAR signals outside the nucleus were excluded, and PAR intensity per nucleus was calculated. In each experiment, >20 cells were examined. *$p < 0.001$, **$p < 0.01$ analyzed with Student's *t* test.

that this response is not seen in WRN-depleted cells (Sharma *et al.*, 2012). This and other studies imply that there is an association between human RecQ helicases and PARP1 in oxidative DNA-damage response. To explore this for RECQL5, we used an immunohistological method to determine cellular PAR activation in HeLa RECQL5-depleted and control cells (Figure 4A). Knockdown and control cells were treated with H_2O_2, fixed, and probed with PAR-specific antibodies, and their immunofluorescence was analyzed by confocal

microscopy. The nuclear PAR intensities were quantified and are shown in Figure 4E. As shown in Figure 4, C and E, PAR immunoreactivity was significantly higher in RECQL5-knockdown than in scrambled control cells. ShRECQL5-1 and shRECQL5-2 cells without treatment showed 1.1- and 1.8-fold higher PAR, respectively, than control cells without treatment, whereas after exposure to H_2O_2, shRECQL5-1 and shRECQL5-2 cells had 1.3- and 1.9-fold higher PAR, respectively, than control cells. In addition, PAR levels were increased in all cells in response to H_2O_2 exposure: treated control cells show 1.2-fold higher PAR than untreated controls, treated shRECQL5-1 cells show 1.4-fold higher PAR than untreated shRECQL5-1, and treated shRECQL5-2 cells show 1.3-fold higher PAR than untreated shRECQL5-2. Collectively, our results suggest that depletion of RECQL5 is associated with an accumulation of DNA damage and lower efficiency of SSBR (Figure 1, G–I).

To compare the roles of RECQL5 and WRN in isogenic cell backgrounds, we performed similar experiments to evaluate whether WRN knockdown in HeLa cells influenced PARP1 activity and cellular PAR after exposure to hydrogen peroxide. First, the efficacy of lentivirus-mediated shRNA knockdown of WRN (shWRN) was confirmed by Western blot (Figure 4B). WRN-depleted and control cells were exposed to H_2O_2 and analyzed by immunofluorescence. The results showed that WRN knockdown had no apparent effect on cellular PAR (Figure 4, D and E). However, PAR did increase in shWRN cells exposed to H_2O_2 (treated cells show 1.3-fold higher PAR than untreated cells; Figure 4, D and E). A significant difference between RECQL5-depleted and WRN-depleted cells, however, is in the PAR levels of untreated cells (Figure 4, C–E).

Expression levels of the BER-related genes in RECQL5-knockdown cells

RECQL5 interacts physically with RNAP II (Aygun *et al.*, 2008; Izumikawa *et al.*, 2008; Islam *et al.*, 2010; Kanagaraj *et al.*, 2010; Li *et al.*, 2011), leading to the speculation that RECQL5 may modulate gene expression. Thus we tested whether RECQL5 might regulate transcription of BER/SSBR genes and thereby indirectly alter the efficiency of BER/SSBR. To address this question, we measured BER gene expression levels by quantitative PCR (qPCR) in RECQL5-knockdown and scrambled control cells. We conducted knockdown in two cellular backgrounds—HeLa cervical and HCT116 colorectal carcinoma cells. In this experiment, HeLa cells treated with shRECQL5-1 and shRECQL5-2 showed ~40 and 70% decrease, respectively, in RECQL5 transcript levels (Figure 5A), whereas HCT116 cells treated with shRECQL5-2 showed ~70% decrease in RECQL5 mRNA (Figure 5D).

We evaluated by qPCR the expression levels of 10 key BER genes (*NEIL1*, *NTH1*, *OGG1*, *APE1*, *POL* β, *FEN1*, *LIG1*, *LIG3*, *XRCC1*, and *PARP1*) in RECQL5-knockdown relative to scrambled control cells. The depletion of shRECQL5 in HeLa cells caused *XRCC1* to be strongly down-regulated to 40–45% of control levels and *PARP1* to be moderately down-regulated to ~70% of control. Smaller effects were observed for *OGG1*, *LIG3*, and *FEN1* (80–90%) and *POL* β and *NEIL1* (90–95%; Figure 5B). Western blots also showed that XRCC1 and PARP1 protein levels were decreased in HeLa shRECQL5-1 and shRECQL5-2 cells (Figure 5C).

Similar results were obtained in HCT116 cells expressing shRECQL5-2. *XRCC1* expression was most down-regulated (25% of control cells). *PARP1* expression was 40% of control (Figure 5E). *FEN1* expression was ~60% of the scrambled control, *POL* β and *NTH1* were 70% of control, and APE1 and *LIG3* were 80% of control cells (Figure 5E). Western blot also confirmed that XRCC1 and PARP1 protein levels were significantly decreased in HCT116 shRECQL5-2 cells (Figure 5F). These results indicate that depletion of RECQL5 caused a significant decrease in expression of XRCC1 and PARP1, which could contribute to BER deficiency.

It is known that expression of many genes can vary, depending on the growth state and/or the cell cycle stage. Therefore we asked whether the decrease in expression of BER genes was dependent on cell cycle and/or growth status of the cells. It was reported that XRCC1 gene expression is regulated with cell cycle status and increases in S phase (Jin *et al.*, 2011), whereas RECQL5 is constitutively expressed (Kitao *et al.*, 1998). We recently showed that the number of S-phase cycling cells in asynchronous populations of RECQL5-depleted cells was similar to that of the shScrambled controls (Ramamoorthy *et al.*, 2012). This would indicate that the down-regulation of XRCC1 in RECQL5-depleted cells is cell cycle independent. To confirm this hypothesis, we analyzed the cell cycle components of asynchronous HeLa RECQL5-depleted cells while simultaneously measuring XRCC1 expression levels by qPCR and Western blot. As shown in Figure 6A, the proportion of cells in S phase was not significantly different when comparing shRECQL5-1 (13.2%), shRECQL5-2 (14.7%), and shScrambled control cells (15.1%). Of importance, the decrease in *XRCC1* expression and protein levels was consistently observed in the cells used for the cell cycle analysis (Figure 6, B and C). Thus we conclude that the down-regulation of XRCC1 observed was caused by RECQL5 depletion, independent of cell cycle regulation.

DISCUSSION

This study characterizes the effect of shRNA-mediated depletion of RECQL5 on cellular BER/SSBR. The results show that depletion of RECQL5 causes increased sensitivity to oxidative stress, higher levels of endogenous DNA damage, and more poly(ADP-ribosyl)ated products. Our results suggest that in human cells RECQL5 plays a significant role in regulating BER and/or SSBR, both directly and indirectly. Consistent with our results, studies in *Drosophila* indicated that DNA strand breaks (both SSBs and DSBs) accumulate in RECQL5 mutants (Nakayama *et al.*, 2009). Recql5 deletion in mouse cells resulted in elevated sister chromatid exchange, a phenomenon associated with increased SSBs, yet no significant difference in cell survival was observed after treatment with methyl methanesulfonate, an agent that creates base modifications that are substrates for BER (Hu *et al.*, 2009). These seemingly conflicting observations may be due to the differences between human and mouse cells.

We found that RECQL5, but not other human RECQ helicases, accumulates at laser-induced SSBs (Figure 2) and that GFP-RECQL5 is recruited to these DNA lesions later than GFP-XRCC1. This finding suggests a role for RECQL5 in the later steps of BER/SSBR and is in accord with previous observations showing that RECQL5 interacts with proliferating cell nuclear antigen (PCNA) and FEN1, two proteins that participate in long-patch BER (Kanagaraj *et al.*, 2006; Speina *et al.*, 2010). Moreover, DNA LIG3 and XRCC1 are recruited rapidly to the microirradiated sites of DNA, whereas DNA LIG1 and PCNA are recruited slowly (Mortusewicz *et al.*, 2006). A recent study also showed that POL β is recruited to the damaged site earlier than FEN1 (Asagoshi *et al.*, 2010). Collectively, XRCC1, LIG3, and POL β appear to be early responders to the SSBs, whereas RECQL5, FEN1, LIG1, and PCNA are late responders. Thus our observations are commensurate with a role for RECQL5 in the late steps of long-patch BER. Our previous findings that RECQL5 colocalizes with FEN1 after oxidative stress and DNA damage also support this notion (Speina *et al.*, 2010).

Significantly, RECQL5-depleted cells, but not WRN-depleted cells, have higher PAR levels than control cells in the absence of

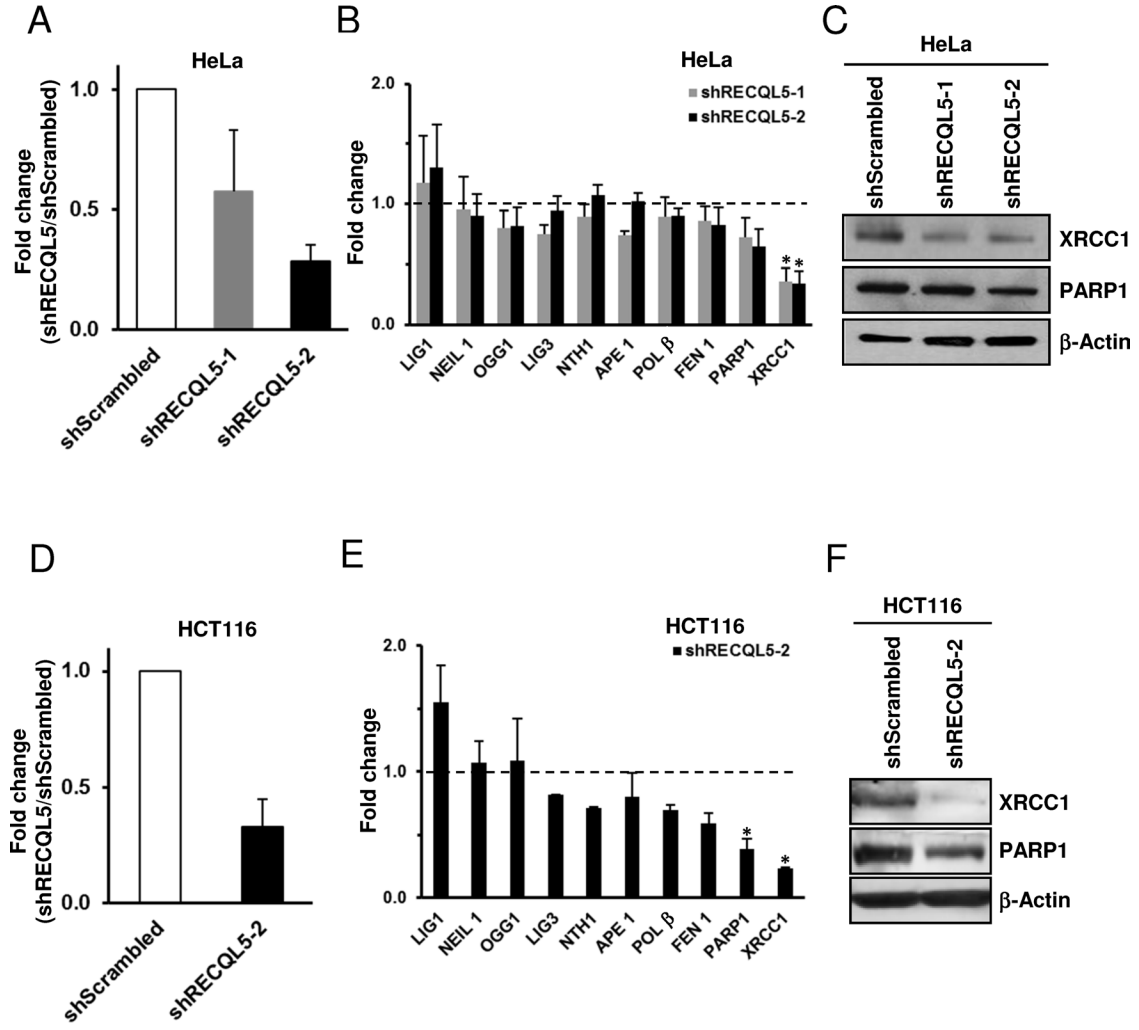

FIGURE 5: BER genes are down-regulated in RECQL5-knockdown cells. (A) Knockdown of RECQL5 using two independent constructs in HeLa cells was confirmed by qPCR. Data were referred from Ramamoorthy *et al.* (2012). (D) Knockdown of RECQL5 in HCT116 cells expressing shRECQL5-2 was confirmed by qPCR. Comparison of the BER-related gene expressions between RECQL5-knockdown and shScrambled control cells in HeLa (B) and in HCT116 (E). ShRECQL5-1 is represented by gray bars, and shRECQL5-2 is represented by black bars. The following were examined: APE1, apurinic endonuclease 1; FEN1, flap endonuclease 1; LIG1, ligase 1; LIG3, ligase 3; NEIL1, nei endonuclease VIII-like 1; NTH1, endonuclease III homologue 1; OGG1, 8-oxoguanine DNA glycosylase; PARP1, poly(ADP-ribose) polymerase 1; POL β, DNA polymerase β; XRCC1, x-ray repair cross-complementing protein 1. At least three biologically independent RNA samples were examined, and error bars represent ± SD. Western blotting shows the comparison of the expression levels of XRCC1 and PARP1 proteins between RECQL5 knockdown and scrambled control cells in HeLa (C) and in HCT116 (F). Experiments were performed at least three times using biologically independent samples, and representative images are shown. *$p < 0.001$ analyzed with Student's *t* test ($n = 3$).

oxidative stress (Figure 4, C and D). The results with WRN-depleted cells differ from a previous report showing that WS patient cells have a defect in PAR synthesis (von Kobbe *et al.*, 2003). This could reflect differences in WRN expression between WRN-depleted and WS patient cells and/or be due to different concentrations of peroxide used (100 vs. 500 μM H_2O_2). In this study, all cells showed elevated PAR after exposure to H_2O_2 when compared with the corresponding untreated cells (Figure 4, C–E), but depletion of RECQL5 resulted in higher PAR immunoreactivity than depletion of WRN. A recent report showed that RECQL1-depleted cells also display increased PAR, specifically in response to H_2O_2 treatment (Sharma *et al.*, 2012). The difference between RECQL5-depleted and RECQL1-depleted cells is in the basal PAR level after gene depletion. We found that RECQL5-depleted cells without any stresses exhibit significantly higher PAR levels than control cells, whereas RECQL1-depleted and WS patient cells show no significant difference in PAR levels as compared with control cells under unstressed conditions (Sharma *et al.*, 2012). Because RECQL5-depleted cells show inefficient BER/SSBR, we propose that RECQL5 is necessary for the repair of endogenous DNA damage. This conclusion is consistent with the results of the alkaline comet assay showing accumulation of endogenous DNA damage in RECQL5-depleted cells (Figure 1, H and I). The idea of defective BER/SSBR is also consistent with the persistence of GFP-XRCC1 foci in RECQL5-depleted cells (Figure 3).

We observed that RECQL5 affects the expression level of BER/SSBR genes, especially XRCC1 and PARP1, potentially indirectly modulating the efficiency of BER/SSBR (Figure 5). Both XRCC1 and

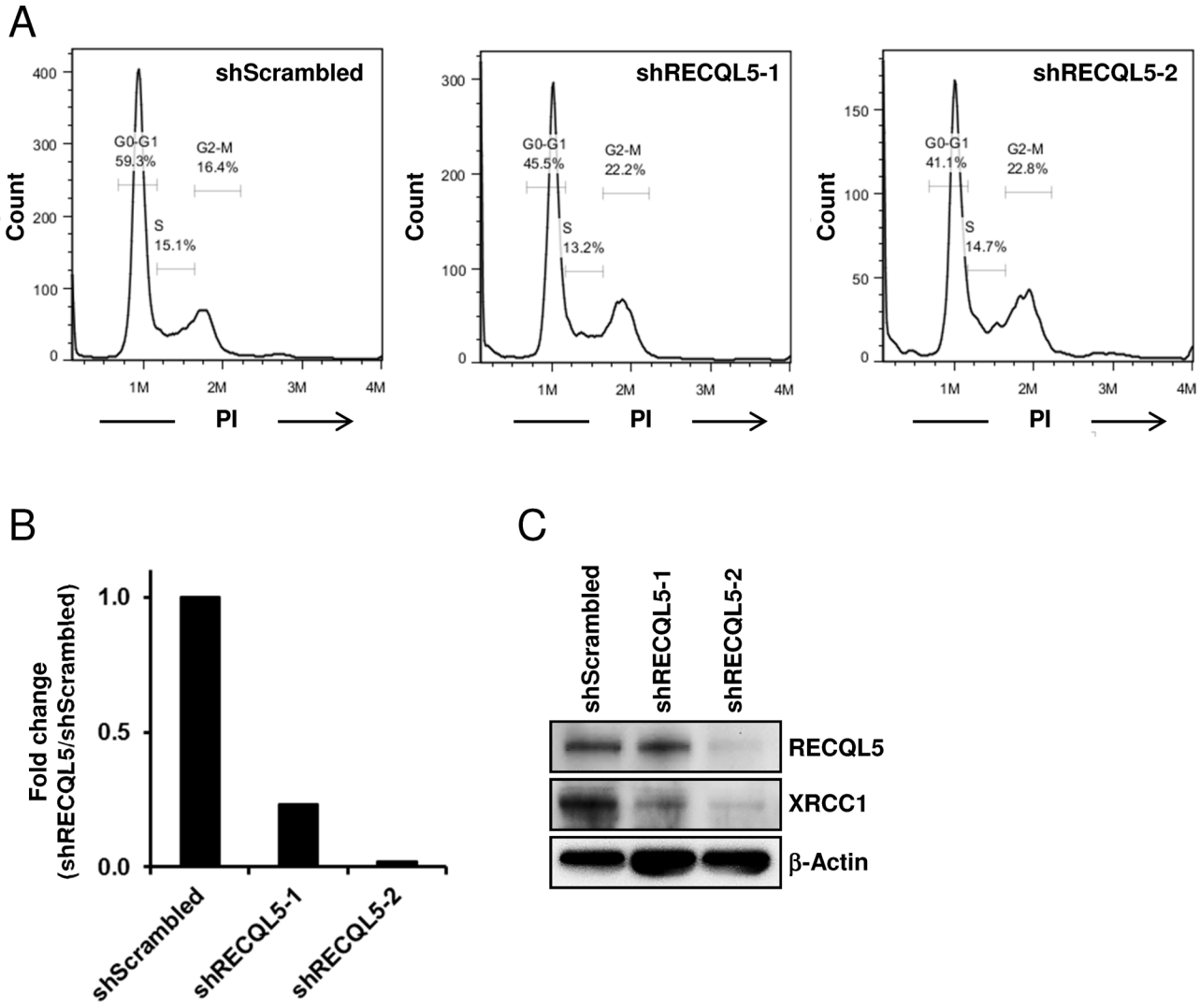

FIGURE 6: RECQL5 is required for XRCC1 gene expression. (A) Cell cycle profiles of asynchronous HeLa cells stably expressing shScrambled, shRECQL5-1, and shRECQL5-2. the *x*- and *y*-axes indicate the DNA content measured by the intensity of propidium iodide staining and the number of cell counts, respectively. Percentage of the cells in each cell cycle stage (G1, S, G2/M) is represented on the histograms. (B) qPCR analysis of XRCC1 mRNA. Same cells for cell cycle analysis in A were used. The total RNA was extracted, cDNA was synthesized, and qPCR was performed as described in *Materials and Methods*. (C) Western blot analysis of XRCC1 protein levels. Same cells for cell cycle analysis in A were used. Cell extracts were prepared and Western blot was conducted as described in *Materials and Methods*.

PARP1 are known to play important roles in BER/SSBR (Caldecott, 2008). For example, a deficiency in XRCC1 and PARP1 inhibition resulted in reduced SSBR, increased sensitivity to DNA-damaging agents, and elevated sister chromatid exchange (Thompson and West, 2000; Godon *et al.*, 2008). *XRCC1* gene expression is regulated by E2F1 and increases in S phase (Jin *et al.*, 2011). Our results indicate that XRCC1 down-regulation occurs after RECQL5 depletion and is independent of the cell cycle status of RECQL5-depleted cells, suggesting that RECQL5 is required for normal XRCC1 expression. Moreover, XRCC1 stimulates the activities of DNA glycosylases, including OGG1 and NEIL1 (Campalans *et al.*, 2005); thus a significant decrease of XRCC1 in RECQL5-depleted cells may cause a more global reduction of SSBR/BER. In addition, we also observed small down-regulation of other BER genes. Because deletion of most of the BER genes, such as APE1/HAP1 (Xanthoudakis *et al.*, 1996), POL β (Cabelof *et al.*, 2003), FEN1 (Larsen *et al.*, 2003), XRCC1 (Tebbs *et al.*, 1999), LIG1 (Bentley *et al.*, 1996), and DNA LIG3 (Puebla-Osorio *et al.*, 2006), results in embryonic lethality, decreased expression of other BER genes could induce further deficiency of BER/SSBR.

RECQ helicases play diverse roles in the maintenance of genome stability. As mentioned, RECQL5 is believed to play a role mainly in RNAP II transcription and DNA recombination. However, it also modulates the activity and expression of multiple proteins in the BER/SSBR pathway. The proposed involvement of RECQL5 in BER is not unique among the RECQ helicases because BLM, WRN, RECQL4, and RECQL1 also play roles in this pathway (Szekely *et al.*, 2005; Harrigan *et al.*, 2006; Schurman *et al.*, 2009; Sharma *et al.*, 2012). Thus human RECQ helicases can affect BER/SSBR in complementary and overlapping roles. In short, the strand displacement DNA synthesis activity of POL β is stimulated by BLM, WRN, and RECQL4 (Harrigan *et al.*, 2003; Schurman *et al.*, 2009). APE1 endonuclease activity is stimulated by RECQL4 (Schurman *et al.*, 2009), whereas neither of these enzymatic activities is stimulated by

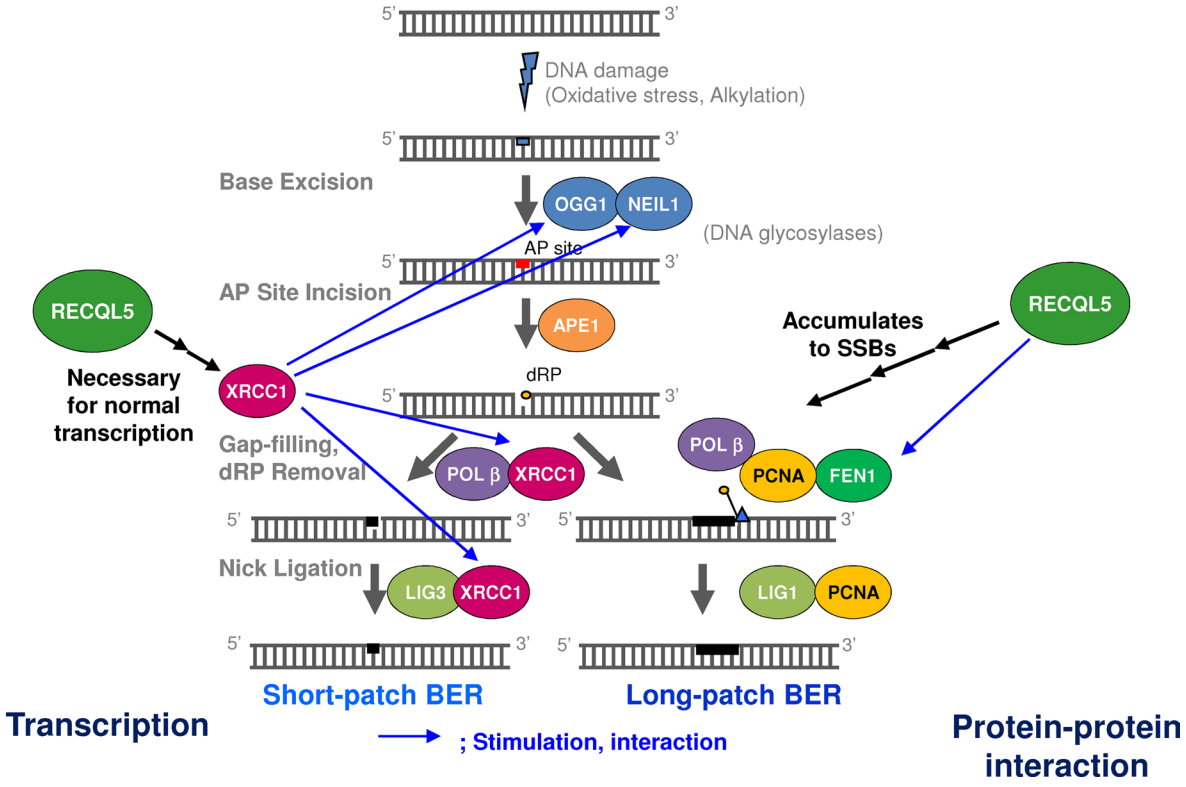

FIGURE 7: Role of RECQL5 in base excision repair. Left, the effect of shRNA-mediated depletion of RECQL5 on BER . Middle, schematic representation of the steps in the BER pathway. Right, protein–protein interactions between BER and its accessory proteins and RECQL5, RECQL4, and WRN. In brief, depletion of RECQL5 results in a lower level of XRCC1 mRNA, which could indicate that RECQL5 (when present at a wild-type concentration) stimulates transcription of XRCC1. RECQL5 is also normally recruited to laser-irradiated SSBs after XRCC1 is recruited to these DNA lesions. Taken together, these data suggest that RECQL5 may directly influence the late stage of BER.

RECQL5 (Speina *et al.*, 2010). FEN1 activity is modulated by BLM, WRN, RECQL4, and RECQL5 (Brosh *et al.*, 2001; Sharma *et al.*, 2004b; Schurman *et al.*, 2009; Speina *et al.*, 2010). FEN 1 is a multifunctional protein, playing roles in homologous recombination, lagging-strand DNA replication, and long patch BER (Lieber, 1997; Shen *et al.*, 2005; Saharia *et al.*, 2008). Thus a general functional interaction exists between RECQ helicases and FEN1 that may be important to all of these processes (Speina *et al.*, 2010). Figure 7 details how RECQL5 interacts with the BER/SSBR pathway at the different stages discussed. Its distinct function among RECQ helicases is that the RECQL5 plays a role as a modulator of transcription in relation to BER/SSBR (Figure 7). RECQL5 is the one human RECQ helicase expressed independently of the cell cycle, and this enzyme appears to play a specialized role in the repair of endogenous DNA damage. Thus we conclude that human RECQ helicases have common roles as modulators of the BER/SSBR pathways while also maintaining unique functions in DNA and RNA metabolism.

MATERIALS AND METHODS

Cells and cell line construction

HeLa and HCT116 cells were purchased from the American Type Culture Collection (ATCC; Manassas, VA) and grown according to their protocols. HEK 293T (ATCC) used for generating lentivirus was cultured in DMEM media supplemented with 10% Hyclone-characterized fetal bovine serum (FBS). Two independent stable knockdown cells for RECQL5 (shRECQL5-1 and shRECQL5-2) were generated as described previously (Ramamoorthy *et al.*, 2012). Briefly, the pLKO.1 vector harboring an shRNA construct targeting human RECQL5 was obtained from Sigma-Aldrich (St. Louis, MO). The construct shRECQL5-1 targets the 3′ untranslated region, 5′-CCGGGCCTTGTGTTTAGACCTGGATCTCGAGATCCAGGTCTAAACACAAGGCTTTTTG-3′; shRECQL5-2 targets the coding region, 5′-CCGGCCCTAAAGGTACGAGTAAGTTCTCGAGAACTTACTCGTACCTTTAGGGTTTTTG-3′. A construct expressing random (i.e., scrambled) shRNA was purchased from Addgene (Cambridge, MA; deposited by the Sabatini lab). Second-generation vesicular stomatitis virus G (VSV-G) pseudotyped lentiviruses were generated by transiently cotransfecting HEK293T cells with the following three plasmids: one 10-cm dish with 50–60% confluent HEK293T cells was transfected with 5 μg of lentiviral vector, 2.5 μg of pCMV ΔR8.2, and 2.5 μg of pCMV VSV-G using FuGENE 6 (Roche, Indianapolis, IN). Supernatants were collected 48 h after transfection, pooled, and frozen at –80°C. For lentiviral transduction, 2×10^5 cells were seeded in 10-cm culture plates and transduced the following day with appropriate lentivirus. At 48 h after transduction, the cells were split and then selected and maintained on media containing 2 μg/ml puromycin. Stable WRN knockdown cells were generated using a similar procedure and an shRNA targeting the coding region of WRN (shWRN; 5′-CCGGCCTGTTTATGTAGGCAAGATTCTCGAGAATCTTGCCTACATAAACAGGTTTTT-3′). Primers were purchased from Sigma-Aldrich.

Western blot

Cells were harvested after 2 d of selection and were lysed in RIPA buffer (50 mM Tris-HCl, pH 8.0, 150 mM NaCl, 0.1% SDS, and 0.5% sodium deoxycholate) supplemented with 1× protease and

phosphatase inhibitors (Roche). Protein concentrations were determined using a protein assay kit manufactured by Bio-Rad (Hercules, CA) based on the Bradford method. We applied 30 µg of total protein per sample to precast 4–12% SDS-polyacrylamide gels (Invitrogen, Carlsbad, CA), transferred to them to polyvinylidene fluoride membrane (Invitrogen), and probed them with the following antibodies: PARP1 (F-2, mouse, 1:500; Santa Cruz Biotechnology, Santa Cruz, CA), poly(ADP-ribose) (51-8114KC, rabbit, 1:1000; BD Biosciences, San Diego, CA), XRCC1 (H-300, rabbit, 1:1000; Santa Cruz Biotechnology), RECQL5 (custom rabbit, 1:1000; Ramamoorthy *et al.*, 2012), WRN (custom mouse; Opresko *et al.*, 2002), 1:1000), and β-actin (Ac-15, mouse, 1:10,000; Sigma-Aldrich).

Cytotoxicity assay

After 2 d of selection, 5000 cells were seeded in triplicate in 96-well plates 1 d before treatment with menadione or hydrogen peroxide. Cells were then treated with menadione (0.5, 1, 2, 5, 15, 25 µM) for 1 h or with hydrogen peroxide (2, 5, 10, 20, 50, 100 µM) for 15 min. The media containing DNA-damaging agents were removed and washed with media, and cells were grown in DMEM supplemented with 10% FBS for 1 d (24 h). Viability was quantified using Cell Counting Kit-8 (Dojindo, Rockville, MD) following manufacturer's protocol. Briefly, cells were mixed with 10 µl of WST-8 solution and were incubated for 2 h, and the absorbance was measured on a Bio-Rad microplate spectrophotometer. Cytotoxicity was proportional to the absorbance at 450 nm (reference at 650 nm) as a measure of WST-8 formazan dye generated by cellular dehydrogenases and was calculated against that measured for untreated controls.

HPLC/electrochemical detection analysis

Quantification of 8-oxoguanine was performed as described previously (Shigenaga *et al.*, 1990; Anson *et al.*, 2000). DNA was digested/cleaved with nuclease P1 and alkaline phosphatase (Boehringer Mannheim, Mannheim, Germany), and nucleosides were purified by filtration through a 0.22-µm filter and a 30-kDa exclusion gel filtration spin column (Shigenaga *et al.*, 1990). Buffers included desferal (1 mM) to chelate iron and minimize oxidative damage during purification.

Nucleosides were separated on a C-8 column (YMC, Wilmington, NC) with isocratic elution (1 ml/min for 30 min) and mobile-phase 100 mM sodium acetate (Sigma-Aldrich), pH 5.15, and 5% methanol (Fisher Scientific International, Hampton, NH). The 8-oxo-dG and 2-deoxyguanosine (dG) were detected electrochemically using a four-channel CoulArray (ESA, Chelmsford, MA). Channels were set at 285 and 400 mV to detect 8-oxo-dG and at 800 and 900 mV to detect dG. Samples were analyzed twice, and peaks were identified by retention time, ratios, and comparison to 2′-deoxyguanosine (Sigma-Aldrich) and 8-oxo-dG standards (ESA). Standard curves were prepared spectrophotometrically using $\varepsilon = 11{,}300$ at 295 nm for 8-oxo-dG and $\varepsilon = 13{,}000$ at 254 nm for dG. The amount of 8-oxo-dG per 10^5 dG was calculated and converted to 8-oxo-dG per 10^6 dN by multiplying by a factor of 2.2. At least two biologically independent DNA samples were used for measurements and analysis.

Alkaline comet assay

The alkaline comet assay was performed as described previously with a slight modification (Morris *et al.*, 1999). Approximately 1 million cells per culture were washed with cold phosphate-buffered saline (PBS) and harvested in 500 µl of PBS. A 10-µl aliquot was mixed with 75 µl of prewarmed 0.5% low–melting point agarose and spread onto an agarose-coated glass slide. A coverslip was added to the slide, and the slide was placed on an ice-chilled aluminum tray for 5 min. The coverslip was removed, another 75 µl of low–melting point agarose was added, a coverslip was added, and the slide was placed on the chilled aluminum tray for 5 min. The coverslip was removed, and the slide was incubated in lysis buffer (2.5 M NaCl, 100 mM EDTA, 10 mM Tris, and 1% Triton X-100) for at least 4 h (or overnight). The slides were washed three times with neutralization buffer (0.4 M Tris, pH 7.4) for 10 min, preincubated with enzyme reaction buffer (10 mM 4-(2-hydroxyethyl)-1-piperazineethanesulfonic acid–KOH, 100 mM KCl, 10 mM EDTA, 0.1 mg/ml bovine serum albumin, pH 7.4) for 10 min, and incubated with 8 U (in 100-µl volume) of Fpg (New England BioLabs, Ipswich, MA) at 37°C for 1 h. Fpg-treated and untreated slides were rinsed with alkali buffer (300 mM NaOH and 1 mM EDTA; pH 12.1) for 20 min to denature DNA. Electrophoresis was performed at 25 V for 15 min, and the slides were dehydrated in 100% ethanol. The slides were stained with ethidium bromide (10 ng/ml). Images were acquired under epifluorescence illumination using a Zeiss Axiovert microscope (Zeiss, Jena, Germany) and analyzed using Komet 5.5 software (Kinetic Imaging, Nottingham, United Kingdom). More than 100 cells were analyzed in each experiment, and experiments were repeated three times using biologically independent samples.

Confocal laser scanning microscopy

We used a Nikon Eclipse 2000E spinning disk confocal microscope (Nikon, Melville, NY) with five laser imaging modules and a charge-coupled device camera (Hamamatsu, Tokyo, Japan). The setup integrated a Stanford Research Systems (SRS) NL100 nitrogen laser by Micropoint ablation system (Photonics Instruments, St. Charles, IL). Site-specific DNA damage was induced using the SRS NL100 nitrogen laser was passed through a dye cell to emit at 435 nm. The power of the laser was attenuated through Volocity-5 (PerkinElmer, Waltham, MA) in terms of percentage intensity. Positions internal to the nuclei of live HeLa cells transfected with GFP-tagged plasmids were targeted via a 40× oil objective lens. The cells were targeted at 3% laser intensity, and the images were captured at different time points and analyzed using Volocity-5 software. Experiments were performed using an environmental chamber attached to the microscope to maintain the normal atmosphere of the cells (37°C and 5% CO_2).

GFP-tagged RECQL5, WRN, XRCC1, and 53BP1 were constructed previously (von Kobbe and Bohr, 2002; Fan *et al.*, 2004; Singh *et al.*, 2010; Popuri *et al.*, 2012).

Immunofluorescence

Exponentially growing cells were plated on Lab-Tek II chambered glass slides (Thermo-Fisher Scientific, Waltham, MA) and treated with 100 µM H_2O_2 (Sigma-Aldrich) in DMEM or DMEM as a control for 15 min. After treatment, cells were fixed and treated with antibodies. The primary antibody was rabbit anti-poly(ADP-ribose) (51-8114KC, 1:500; BD Biosciences), and secondary antibody was donkey anti-rabbit Alexa Fluor 488, 1:1000. Images were captured with a Nikon Eclipse TE2000 confocal microscope and analyzed using Volocity-5 software.

Quantitative real-time PCR

Total RNA was extracted from RECQL5-knockdown and control cells after 2 d of selection using TRIzol (Invitrogen, Carlsbad, CA). Extracted RNA was quantified using a NanoDrop ND-1000 Spectrophotometer (NanoDrop, Wilmington, DE), and the quality of the RNA was assessed by gel electrophoresis. The cDNA was synthesized from 0.5 µg or 1.0 µg of total RNA using iScript cDNA Synthesis Kit (Bio-Rad). qPCR was performed using IQ SYBR Green Supermix (Bio-Rad)

and/or TaqMan Gene Expression Assay Kit (Applied Biosystems, Foster City, CA) with primer sets targeting BER-related genes: APE1, FEN1, LIG1, LIG3, NEIL1, NTH1, OGG1, PARP1, POL β, and XRCC1. RECQL5 mRNA level was also quantified. The glyceraldehyde-3-phosphate dehydrogenase gene was used as an internal control. The real-time PCR for each RNA sample was performed in triplicate, and at least three independent biological samples were examined.

Flow cytometry

To measure cell cycle status, cells were harvested by trypsinization and combined with the media from the cell cultures containing floating (mitotic) cells to ensure that the analysis was unbiased by excluding M-phase events. After a brief centrifugation, the cell pellets were resuspended in 70% ethanol and frozen at −20°C overnight. The fixed cells were washed and incubated with propidium iodide solution (50 μg/ml propidium iodide in the presence of RNase). The samples were analyzed in a fluorescence-activated cell sorter (Accuri C6; BD Accuri Cytometers, Ann Arbor, MI). The percentage of cells in the G0/G1, S, and G2/M phases of the cell cycle was measured using Flowjo software (TreeStar, Ashland, OR) and corrected for the effects of debris and doublets by software algorithms.

ACKNOWLEDGMENTS

We thank Tomasz Kulikowicz for the GFP-tagged RECQL5 plasmid. We also thank Jenq-Lin Yang, Marie Rossi, and Christopher Dunn for technical assistance. We thank Avik K. Ghosh and Morten Scheibye-Knudsen for critically reading the manuscript. This research was supported by funds from the Intramural Research Program of the National Institutes of Health, National Institute on Aging.

REFERENCES

Ahn B, Harrigan JA, Indig FE, Wilson DM III, Bohr VA (2004). Regulation of WRN helicase activity in human base excision repair. J Biol Chem 279, 53465–53474.

Anson RM, Hudson E, Bohr VA (2000). Mitochondrial endogenous oxidative damage has been overestimated. FASEB J 14, 355–360.

Asagoshi K *et al*. (2010). DNA polymerase beta-dependent long patch base excision repair in living cells. DNA Repair (Amst) 9, 109–119.

Aygun O, Svejstrup J, Liu YL (2008). A RECQ5-RNA polymerase II association identified by targeted proteomic analysis of human chromatin. Proc Natl Acad Sci USA 105, 8580–8584.

Bentley D, Selfridge J, Millar JK, Samuel K, Hole N, Ansell JD, Melton DW (1996). DNA ligase I is required for fetal liver erythropoiesis but is not essential for mammalian cell viability. Nat Genet 13, 489–491.

Bohr VA (2008). Rising from the RecQ-age: the role of human RecQ helicases in genome maintenance. Trends Biochem Sci 33, 609–620.

Brosh RM Jr, Bohr VA (2007). Human premature aging, DNA repair and RecQ helicases. Nucleic Acids Res 35, 7527–7544.

Brosh RM Jr, von Kobbe C, Sommers JA, Karmakar P, Opresko PL, Piotrowski J, Dianova I, Dianov GL, Bohr VA (2001). Werner syndrome protein interacts with human flap endonuclease 1 and stimulates its cleavage activity. EMBO J 20, 5791–5801.

Cabelof DC, Guo Z, Raffoul JJ, Sobol RW, Wilson SH, Richardson A, Heydari AR (2003). Base excision repair deficiency caused by polymerase beta haploinsufficiency: accelerated DNA damage and increased mutational response to carcinogens. Cancer Res 63, 5799–5807.

Caldecott KW (2008). Single-strand break repair and genetic disease. Nat Rev Genet 9, 619–631.

Campalans A, Marsin S, Nakabeppu Y, O'Connor TR, Boiteux S, Radicella JP (2005). XRCC1 interactions with multiple DNA glycosylases: a model for its recruitment to base excision repair. DNA Repair (Amst) 4, 826–835.

Chu WK, Hickson ID (2009). RecQ helicases: multifunctional genome caretakers. Nat Rev Cancer 9, 644–654.

Das A *et al*. (2007). The human Werner syndrome protein stimulates repair of oxidative DNA base damage by the DNA glycosylase NEIL1. J Biol Chem 282, 26591–26602.

Dietschy T, Shevelev I, Stagljar I (2007). The molecular role of the Rothmund-Thomson-, RAPADI. Cell Mol Life Sci 64, 796–802.

Fan J, Otterlei M, Wong HK, Tomkinson AE, Wilson DM III (2004). XRCC1 co-localizes and physically interacts with PCNA. Nucleic Acids Res 32, 2193–2201.

Godon C, Cordelieres FP, Biard D, Giocanti N, Megnin-Chanet F, Hall J, Favaudon V (2008). PARP inhibition versus PARP-1 silencing: different outcomes in terms of single-strand break repair and radiation susceptibility. Nucleic Acids Res 36, 4454–4464.

Golden TR, Hinerfeld DA, Melov S (2002). Oxidative stress and aging: beyond correlation. Aging Cell 1, 117–123.

Haince JF, McDonald D, Rodrigue A, Dery U, Masson JY, Hendzel MJ, Poirier GG (2008). PARP1-dependent kinetics of recruitment of MRE11 and NBS1 proteins to multiple DNA damage sites. J Biol Chem 283, 1197–1208.

Harrigan JA, Opresko PL, von Kobbe C, Kedar PS, Prasad R, Wilson SH, Bohr VA (2003). The Werner syndrome protein stimulates DNA polymerase beta strand displacement synthesis via its helicase activity. J Biol Chem 278, 22686–22695.

Harrigan JA, Wilson DM III, Prasad R, Opresko PL, Beck G, May A, Wilson SH, Bohr VA (2006). The Werner syndrome protein operates in base excision repair and cooperates with DNA polymerase beta. Nucleic Acids Res 34, 745–754.

Heeres JT, Hergenrother PJ (2007). Poly(ADP-ribose) makes a date with death. Curr Opin Chem Biol 11, 644–653.

Hu J, de Souza-Pinto NC, Haraguchi K, Hogue BA, Jaruga P, Greenberg MM, Dizdaroglu M, Bohr VA (2005a). Repair of formamidopyrimidines in DNA involves different glycosylases: role of the OGG1, NTH1, and NEIL1 enzymes. J Biol Chem 280, 40544–40551.

Hu Y *et al.* (2007). RECQL5/Recql5 helicase regulates homologous recombination and suppresses tumor formation via disruption of Rad51 presynaptic filaments. Genes Dev 21, 3073–3084.

Hu Y, Lu X, Barnes E, Yan M, Lou H, Luo G (2005b). Recql5 and Blm RecQ DNA helicases have nonredundant roles in suppressing crossovers. Mol Cell Biol 25, 3431–3442.

Hu Y, Lu X, Zhou G, Barnes EL, Luo G (2009). Recql5 plays an important role in DNA replication and cell survival after camptothecin treatment. Mol Biol Cell 20, 114–123.

Imamura O, Fujita K, Itoh C, Takeda S, Furuichi Y, Matsumoto T (2002). Werner and Bloom helicases are involved in DNA repair in a complementary fashion. Oncogene 21, 954–963.

Islam MN, Fox D III, Guo R, Enomoto T, Wang W (2010). RecQL5 promotes genome stabilization through two parallel mechanisms—interacting with RNA polymerase II and acting as a helicase. Mol Cell Biol 30, 2460–2472.

Izumikawa K *et al*. (2008). Association of human DNA helicase RecQ5beta with RNA polymerase II and its possible role in transcription. Biochem J 413, 505–516.

Jeong YS, Kang Y, Lim KH, Lee MH, Lee J, Koo HS (2003). Deficiency of *Caenorhabditis elegans* RecQ5 homologue reduces life span and increases sensitivity to ionizing radiation. DNA Repair (Amst) 2, 1309–1319.

Jin R, Sun Y, Qi X, Zhang H, Zhang Y, Li N, Ding W, Chen D (2011). E2F1 is involved in DNA single-strand break repair through cell-cycle-dependent upregulation of XRCC1 expression. DNA Repair (Amst) 10, 926–933.

Kanagaraj R, Huehn D, MacKellar A, Menigatti M, Zheng L, Urban V, Shevelev I, Greenleaf AL, Janscak P (2010). RECQ5 helicase associates with the C-terminal repeat domain of RNA polymerase II during productive elongation phase of transcription. Nucleic Acids Res 38, 8131–8140.

Kanagaraj R, Saydam N, Garcia PL, Zheng L, Janscak P (2006). Human RECQ5beta helicase promotes strand exchange on synthetic DNA structures resembling a stalled replication fork. Nucleic Acids Res 34, 5217–5231.

Karmakar P *et al*. (2006). BLM is an early responder to DNA double-strand breaks. Biochem Biophys Res Commun 348, 62–69.

Kitao S, Ohsugi I, Ichikawa K, Goto M, Furuichi Y, Shimamoto A (1998). Cloning of two new human helicase genes of the RecQ family: biological significance of multiple species in higher eukaryotes. Genomics 54, 443–452.

Kitao S, Shimamoto A, Goto M, Miller RW, Smithson WA, Lindor NM, Furuichi Y (1999). Mutations in RECQL4 cause a subset of cases of Rothmund-Thomson syndrome. Nat Genet 22, 82–84.

Lan L, Nakajima S, Komatsu K, Nussenzweig A, Shimamoto A, Oshima J, Yasui A (2005). Accumulation of Werner protein at DNA double-strand breaks in human cells. J Cell Sci 118, 4153–4162.

Larsen E, Gran C, Saether BE, Seeberg E, Klungland A (2003). Proliferation failure and gamma radiation sensitivity of Fen1 null mutant mice at the blastocyst stage. Mol Cell Biol 23, 5346–5353.
Li M, Xu X, Liu Y (2011). The SET2-RPB1 interaction domain of human RECQ5 is important for transcription-associated genome stability. Mol Cell Biol 31, 2090–2099.
Lieber MR (1997). The FEN-1 family of structure-specific nucleases in eukaryotic DNA replication, recombination and repair. Bioessays 19, 233–240.
Lindor NM, Furuichi Y, Kitao S, Shimamoto A, Arndt C, Jalal S (2000). Rothmund-Thomson syndrome due to RECQ4 helicase mutations: report and clinical and molecular comparisons with Bloom syndrome and Werner syndrome. Am J Med Genet 90, 223–228.
Mailand N, Bekker-Jensen S, Faustrup H, Melander F, Bartek J, Lukas C, Lukas J (2007). RNF8 ubiquitylates histones at DNA double-strand breaks and promotes assembly of repair proteins. Cell 131, 887–900.
Masson M, Niedergang C, Schreiber V, Muller S, Menissier-de Murcia J, de Murcia G (1998). XRCC1 is specifically associated with poly(ADP-ribose) polymerase and negatively regulates its activity following DNA damage. Mol Cell Biol 18, 3563–3571.
Morris EJ, Dreixler JC, Cheng KY, Wilson PM, Gin RM, Geller HM (1999). Optimization of single-cell gel electrophoresis (SCGE) for quantitative analysis of neuronal DNA damage. Biotechniques 26, 282–289.
Mortusewicz O, Rothbauer U, Cardoso MC, Leonhardt H (2006). Differential recruitment of DNA Ligase I and III to DNA repair sites. Nucleic Acids Res 34, 3523–3532.
Nakayama M, Yamaguchi S, Sagisu Y, Sakurai H, Ito F, Kawasaki K (2009). Loss of RecQ5 leads to spontaneous mitotic defects and chromosomal aberrations in *Drosophila melanogaster*. DNA Repair (Amst) 8, 232–241.
Opresko PL, von Kobbe C, Laine JP, Harrigan J, Hickson ID, Bohr VA (2002). Telomere-binding protein TRF2 binds to and stimulates the Werner and Bloom syndrome helicases. J Biol Chem 277, 41110–41119.
Pleschke JM, Kleczkowska HE, Strohm M, Althaus FR (2000). Poly(ADP-ribose) binds to specific domains in DNA damage checkpoint proteins. J Biol Chem 275, 40974–40980.
Popuri V, Croteau DL, Bohr VA (2010). Substrate specific stimulation of NEIL1 by WRN but not the other human RecQ helicases. DNA Repair (Amst) 9, 636–642.
Popuri V, Ramamoorthy M, Tadokoro T, Singh DK, Karmakar P, Croteau DL, Bohr VA (2012). Recruitment and retention dynamics of RECQL5 at DNA double strand break sites. DNA Repair (Amst) 11, 624–635.
Puebla-Osorio N, Lacey DB, Alt FW, Zhu C (2006). Early embryonic lethality due to targeted inactivation of DNA ligase III. Mol Cell Biol 26, 3935–3941.
Ramamoorthy M, Tadokoro T, Rybanska I, Ghosh AK, Wersto R, May A, Kulikowicz T, Sykora P, Croteau DL, Bohr VA (2012). RECQL5 cooperates with topoisomerase II alpha in DNA decatenation and cell cycle progression. Nucleic Acids Res 40, 1621–1635.
Saharia A, Guittat L, Crocker S, Lim A, Steffen M, Kulkarni S, Stewart SA (2008). Flap endonuclease 1 contributes to telomere stability. Curr Biol 18, 496–500.
Schurman SH *et al.* (2009). Direct and indirect roles of RECQL4 in modulating base excision repair capacity. Hum Mol Genet 18, 3470–3483.
Schwendener S, Raynard S, Paliwal S, Cheng A, Kanagaraj R, Shevelev I, Stark JM, Sung P, Janscak P (2010). Physical interaction of RECQ5 helicase with RAD51 facilitates its anti-recombinase activity. J Biol Chem 285, 15739–15745.
Sharma S, Otterlei M, Sommers JA, Driscoll HC, Dianov GL, Kao HI, Bambara RA, Brosh RM Jr (2004a). WRN helicase and FEN-1 form a complex upon replication arrest and together process branchmigrating DNA structures associated with the replication fork. Mol Biol Cell 15, 734–750.
Sharma S, Phatak P, Stortchevoi A, Jasin M, Larocque JR (2012). RECQ1 plays a distinct role in cellular response to oxidative DNA damage. DNA Repair (Amst) 11, 537–549.
Sharma S, Sommers JA, Wu L, Bohr VA, Hickson ID, Brosh RM Jr (2004b). Stimulation of flap endonuclease-1 by the Bloom's syndrome protein. J Biol Chem 279, 9847–9856.
Shen B, Singh P, Liu R, Qiu J, Zheng L, Finger LD, Alas S (2005). Multiple but dissectible functions of FEN-1 nucleases in nucleic acid processing, genome stability and diseases. Bioessays 27, 717–729.
Shigenaga MK, Park JW, Cundy KC, Gimeno CJ, Ames BN (1990). In vivo oxidative DNA damage: measurement of 8-hydroxy-2'-deoxyguanosine in DNA and urine by high-performance liquid chromatography with electrochemical detection. Methods Enzymol 186, 521–530.
Shimamoto A, Nishikawa K, Kitao S, Furuichi Y (2000). Human RecQ5beta, a large isomer of RecQ5 DNA helicase, localizes in the nucleoplasm and interacts with topoisomerases 3alpha and 3beta. Nucleic Acids Res 28, 1647–1655.
Singh DK, Ghosh AK, Croteau DL, Bohr VA (2012). RecQ helicases in DNA double strand break repair and telomere maintenance. Mutat Res 736, 15–24.
Singh DK, Karmakar P, Aamann M, Schurman SH, May A, Croteau DL, Burks L, Plon SE, Bohr VA (2010). The involvement of human RECQL4 in DNA double-strand break repair. Aging Cell 9, 358–371.
Speina E, Dawut L, Hedayati M, Wang Z, May A, Schwendener S, Janscak P, Croteau DL, Bohr VA (2010). Human RECQL5beta stimulates flap endonuclease 1. Nucleic Acids Res 38, 2904–2916.
Szekely AM, Bleichert F, Numann A, Van KS, Manasanch E, Ben NA, Canaan A, Weissman SM (2005). Werner protein protects nonproliferating cells from oxidative DNA damage. Mol Cell Biol 25, 10492–10506.
Tebbs RS, Flannery ML, Meneses JJ, Hartmann A, Tucker JD, Thompson LH, Cleaver JE, Pedersen RA (1999). Requirement for the Xrcc1 DNA base excision repair gene during early mouse development. Dev Biol 208, 513–529.
Thompson LH, West MG (2000). XRCC1 keeps DNA from getting stranded. Mutat Res 459, 1–18.
von Kobbe C, Bohr VA (2002). A nucleolar targeting sequence in the Werner syndrome protein resides within residues 949–1092. J Cell Sci 115, 3901–3907.
von Kobbe C, Harrigan JA, May A, Opresko PL, Dawut L, Cheng WH, Bohr VA (2003). Central role for the Werner syndrome protein/poly(ADP-ribose) polymerase 1 complex in the poly(ADP-ribosyl)ation pathway after DNA damage. Mol Cell Biol 23, 8601–8613.
Wang W *et al.* (2003). Functional relation among RecQ family helicases RecQL1, RecQL5, and BLM in cell growth and sister chromatid exchange formation. Mol Cell Biol 23, 3527–3535.
Wang X, Lu X, Zhou G, Lou H, Luo G (2011). RECQL5 is an important determinant for camptothecin tolerance in human colorectal cancer cells. Biosci Rep 31, 363–369.
Wilson DM III, Bohr VA (2007). The mechanics of base excision repair, and its relationship to aging and disease. DNA Repair (Amst) 6, 544–559.
Xanthoudakis S, Smeyne RJ, Wallace JD, Curran T (1996). The redox/DNA repair protein, Ref-1, is essential for early embryonic development in mice. Proc Natl Acad Sci USA 93, 8919–8923.
Yano K, Morotomi-Yano K, Wang SY, Uematsu N, Lee KJ, Asaithamby A, Weterings E, Chen DJ (2008). Ku recruits XLF to DNA double-strand breaks. EMBO Rep 9, 91–96.
Yu CE *et al.* (1996). Positional cloning of the Warner's syndrome gene. Science 272, 258–262.